


Quantum Simulation of SU(3) Lattice Yang-Mills Theory at Leading Order in Large- N_c Expansion

Anthony N. Ciavarella^{1,*} and Christian W. Bauer^{1,2,†}

¹Physics Division, Lawrence Berkeley National Laboratory, Berkeley, California 94720, USA

²Department of Physics, University of California, Berkeley, Berkeley, California 94720, USA

 (Received 28 February 2024; revised 26 July 2024; accepted 5 August 2024; published 9 September 2024)

Quantum simulations of the dynamics of QCD have been limited by the complexities of mapping the continuous gauge fields onto quantum computers. By parametrizing the gauge invariant Hilbert space in terms of plaquette degrees of freedom, we show how the Hilbert space and interactions can be expanded in inverse powers of N_c . At leading order in this expansion, the Hamiltonian simplifies dramatically, both in the required size of the Hilbert space as well as the type of interactions involved. Adding a truncation of the resulting Hilbert space in terms of local energy states we give explicit constructions that allow simple representations of SU(3) gauge fields on qubits and qutrits. This formulation allows a simulation of the real time dynamics of a SU(3) lattice gauge theory on a 5×5 and 8×8 lattice on `ibm_torino` with a CNOT depth of 113.

DOI: [10.1103/PhysRevLett.133.111901](https://doi.org/10.1103/PhysRevLett.133.111901)

The real time dynamics of strongly coupled quantum field theories such as quantum chromodynamics (QCD) are relevant to many processes in high energy physics. These include phenomena such as hadronization, jet fragmentation, and the behavior of matter under extreme conditions such as in the early universe. The numerical study of QCD on a lattice using Monte Carlo (MC) integration has enabled precision nonperturbative calculations of a number of observables [1–6]. However, for many observables such as the QCD shear viscosity and inelastic scattering amplitudes, Monte Carlo integration is limited due to a sign problem [7]. Hamiltonian lattice QCD formulations promise to circumvent the sign problem, but are still exponentially difficult to simulate on classical computers. Research in Hamiltonian formulations has gained importance recently due to advances in the development of quantum computers based on a number of different platforms, such as superconducting qubits, trapped ions, and neutral atoms [8–18]. It is anticipated that simulations performed on quantum computers will be able to directly probe real-time dynamics with polynomially scaling computational costs [19–25]. The continuous gauge fields need to be digitized to map them onto a quantum computer’s discrete degrees of freedom. Common basis choices for the Hilbert space of a

lattice gauge theory (LGT) correspond to choosing on each link group elements (magnetic basis) [26–33], group representations (electric basis) [34–63], or a mixture of the two [64–67], and digitizations can be obtained in each of the choices. These formal developments have been used to perform a number of quantum simulations on existing hardware including simulations of the Schwinger model, 1 + 1D QCD, SU(2), and SU(3) gauge theories on small lattices and some discrete groups [30,31,46–52,68–82]. However, most quantum simulations of lattice gauge theories have been restricted to either small systems or one-dimensional systems. Going beyond (1 + 1)D systems is limited by the complexity of implementing plaquette operators which are not present in one spatial dimension.

In this work we will use an electric basis, in which states are labeled by the representation of the gauge group at each link and gauge invariance can be implemented using local constraints that implement Gauss’s law at each lattice site. The electric basis can be digitized by truncating the allowed representations at each link, which amounts to limiting the local energy allowed. This can be done in a way that respects gauge invariance, and gauge invariance can be used to integrate out some unphysical states at the cost of a slight increase in the nonlocality of the Hamiltonian [48].

In this work we add an expansion in the number of colors N_c to the electric basis formulation. It is known that such a $1/N_c$ expansion leads to simplifications in perturbative QCD (for a review, see Refs. [83,84]), and is a crucial ingredient in many calculational frameworks of QCD, most notably the parton shower approximation [85,86]. Combining a large N_c expansion with the lattice formulation of QCD will enable lattice calculations to reproduce the results of these frameworks and determine $1/N_c$

*Contact author: anciovarella@lbl.gov

†Contact author: cwbauer@lbl.gov

Published by the American Physical Society under the terms of the [Creative Commons Attribution 4.0 International license](https://creativecommons.org/licenses/by/4.0/). Further distribution of this work must maintain attribution to the author(s) and the published article’s title, journal citation, and DOI. Funded by SCOAP³.

corrections to them. While the physical value of $N_c = 3$ is not particularly large, such expansions have been shown to be very successful phenomenologically [85–89]. Additionally, the large N_c limit of QCD has been shown to be connected to models of quantum gravity through the AdS/CFT correspondence [90].

The large N_c limit can be understood as a classical limit [91,92] and by expanding in $1/N_c$ more nonclassical features of the theory will be included in the quantum simulation. Note that the classical limit has a degree of freedom for each possible loop on the lattice which limits its applicability to simulating dynamics on classical computers [92–94].

The Kogut Susskind Hamiltonian describing pure SU(3) LGT is given by

$$\hat{H} = \frac{g^2}{2} \sum_{l \in \text{links}} \hat{E}_l^2 - \frac{1}{2g^2} \sum_{p \in \text{plaquettes}} (\square_p + \square_p^\dagger), \quad (1)$$

where g is the strong coupling constant, $\hat{E}_l^2 = \hat{E}_l^c \hat{E}_l^c$ with \hat{E}_l^c the SU(3) chromoelectric field on link l , and \square_p is the trace over color indices of the product of parallel transporters on plaquette p [95–98]. In the electric basis, the Hilbert space on each link is spanned by states $|R, a, b\rangle$ where R is an irreducible representation of SU(3) and a and b label states in the representation R acting from the left and right.

The SU(3) representation at each link on a point-split lattice can be labeled by the two quantum numbers p and q , due to SU(3) being a rank two group. A gauge invariant representation requires representations at each vertex to combine into a singlet. This is most easily accomplished using point-split vertices and requiring that the quantum numbers at each three-point vertex add to zero. This has previously been used in formulations of q -deformed lattice gauge theories [99,100] and is very similar to the approach taken in loop string hadron formulations [41–43,101].

As explained in Appendix A, an alternative labeling of a gauge invariant Hilbert state is obtained by specifying oriented closed loops, denoted by L , and the way the arrows at each link having more than one loop pass through are combined, denoted by a . A basis state can therefore be written as $|\{L_i, a_\ell\}\rangle$. The only physically relevant states have nonzero overlap with those obtained by acting on the electric vacuum state $|0\rangle$ with an operator $\hat{O}_{\{P_p, \bar{P}_p\}}$ containing P_p (\bar{P}_p) powers of the plaquette operator \square_p (\square_p^\dagger) at each plaquette p . While other gauge invariant states do exist, they are in different topological sectors and do not need to be represented on the quantum computer as different topological sectors do not interact. For example, a state with a loop of electric flux winding across the entire lattice has a nontrivial winding number and is not coupled to the electric vacuum. The operator $\hat{O}_{\{P_p, \bar{P}_p\}}$ allows us to define the state

$$|\{P_p, \bar{P}_p\}\rangle = \hat{O}_{\{P_p, \bar{P}_p\}}|0\rangle. \quad (2)$$

As shown in Appendix B, the overlap between $|\{L_i, a_\ell\}\rangle$ and $|\{P_p, \bar{P}_p\}\rangle$ at leading order in large N_c is given by

$$\langle \{L_i, a_\ell\} | \{P_p, \bar{P}_p\} \rangle \propto \prod_i N_c^{1-m_i}, \quad (3)$$

where m_i counts the total number of plaquettes encircled by each loop L_i . Therefore, the only overlap that survives in the large N_c limit is the one with states $|\{L_i, a_\ell\}\rangle$ for which each loop encircles exactly one plaquette, such that all $m_i = 1$. This leads to the final result that in the large N_c limit each state can be specified by the number of single-plaquette loops in the positive and negative direction at each plaquette and a at each link traversed by multiple of these loops. These states are orthonormal to each other, such that the Hilbert space is spanned by the basis

$$\mathcal{H} = \text{span}\{|\{a_\ell, n_p, \bar{n}_p\}\rangle\}. \quad (4)$$

Because of the suppression of larger loops, the dimension of the Hilbert space in the large N_c limit is dramatically reduced. Another important simplification is that in this formulation no virtual point splitting is required.

So far, our discussion has not used any truncation of the Hilbert space. However, a truncation is necessary to map the theory onto the finite dimensional Hilbert space of a quantum computer. As already discussed, a standard way of truncating the Hilbert space is to limit the energy stored in each link of the lattice, which in turn limits the Hilbert space to those states for which the Casimir at each link is below a certain value. This truncation preserves all symmetries of the Hamiltonian, most importantly gauge invariance, which guarantees the truncated theory either to have a lattice spacing that freezes out or goes to a theory with the correct gauge symmetry and matter content in the continuum limit [102]. Simulations of truncated 1 + 1D theories have demonstrated the freezing out of the lattice spacing [103–108], although some infrared properties of the theory can still be recovered [109]. This truncation amounts to limiting the total value of $p + q$ at each link. The simplest nontrivial truncation is to require $p + q \leq 1$ which only includes the fundamental and antifundamental representations. Working to leading order in large N_c , this allows at most one loop excitation at each plaquette. Furthermore, a plaquette can only be excited if all adjacent plaquettes are in the ground state. The only allowed values for $\{n_p, \bar{n}_p\}$ are then $\{0,0\}$, $\{0,1\}$ or $\{1,0\}$, and no specification of a_ℓ is necessary.

The Hilbert space at this truncation can therefore be described by assigning a qutrit to each plaquette in the lattice. The states of the qutrit will be labeled by $|0\rangle$, $|\mathcal{O}\rangle$, and $|\mathcal{U}\rangle$. Physical states are subject to the constraint that neighboring plaquettes are not simultaneously excited. For

example, in a two plaquette system, the states $|\mathcal{U}\rangle|0\rangle$ and $|\mathcal{V}\rangle|0\rangle$ are physical while $|\mathcal{U}\rangle|\mathcal{U}\rangle$ and $|\mathcal{U}\rangle|\mathcal{V}\rangle$ are not, since it would give rise to the common link having $p + q > 1$. Similar constructions have been used to study SU(2) lattice gauge theory in the electric basis on plaquette chains and a hexagonal lattice [50,110–115]. However, note that the basis given here can work in higher spatial dimensions and with periodic boundary conditions as there is no potential double counting of states at this truncation unlike previous work on the hexagonal lattice.

If one works to leading order in $N_c = 3$ and in $2 + 1D$, the electric field operator for a link ℓ lying on plaquettes p and p' at this truncation can be written as

$$\hat{E}_\ell^2 = \frac{4}{3} [|\mathcal{U}\rangle_p \langle \mathcal{U}|_p + |\mathcal{U}\rangle_{p'} \langle \mathcal{U}|_{p'} + (|\mathcal{U}\rangle \leftrightarrow |\mathcal{V}\rangle)], \quad (5)$$

where we have used the full expression of the Casimir of the fundamental representation $C_f = (N_c^2 - 1)/(2N_c) = 4/3$. The plaquette operator at position p is given by

$$\hat{\square}_p = \hat{P}_{0,p+\hat{x}} \hat{P}_{0,p-\hat{x}} \hat{P}_{0,p+\hat{y}} \hat{P}_{0,p-\hat{y}} \times (|\mathcal{U}\rangle_p \langle 0|_p + |\mathcal{U}\rangle_p \langle \mathcal{U}|_p + |0\rangle_p \langle \mathcal{U}|_p), \quad (6)$$

where $\hat{P}_{0,p} = |0\rangle_p \langle 0|_p$ and $p \pm \hat{x}$ ($p \pm \hat{y}$) denotes the plaquette one position away in the x (y) direction.

This Hamiltonian has a charge conjugation (C) symmetry that causes states with the antisymmetric combination $(1/\sqrt{2})(|\mathcal{U}\rangle - |\mathcal{V}\rangle)$ anywhere on the lattice to decouple from the rest of the Hilbert space. This decoupling can be seen by repeated applications of the plaquette operators to the electric vacuum. Explicitly, we have

$$\hat{\square}_p |0\rangle = |\mathcal{U}\rangle + |\mathcal{V}\rangle \\ \hat{\square}_p \frac{1}{\sqrt{2}} (|\mathcal{U}\rangle + |\mathcal{V}\rangle) = \sqrt{2}|0\rangle + \frac{1}{\sqrt{2}} (|\mathcal{U}\rangle + |\mathcal{V}\rangle), \quad (7)$$

so the state $(1/\sqrt{2})(|\mathcal{U}\rangle - |\mathcal{V}\rangle)$ is never coupled to the rest of the Hilbert space. One can therefore perform separate simulations for the C even and odd sector. By assigning $|1\rangle = (1/\sqrt{2})(|\mathcal{U}\rangle \pm |\mathcal{V}\rangle)$, the C (anti)symmetric subspace can be described by assigning a qubit to each plaquette instead of a qutrit. As already mentioned, physical states have the constraint that neighboring qubits cannot both be in the $|1\rangle$ state. With this encoding, the Hamiltonian for the C even sector is given by

$$\hat{H} = \sum_p \left(\frac{8}{3} g^2 - \frac{1}{2g^2} \right) \hat{P}_{1,p} \\ - \frac{1}{g^2 \sqrt{2}} \hat{P}_{0,p+\hat{x}} \hat{P}_{0,p-\hat{x}} \hat{P}_{0,p+\hat{y}} \hat{P}_{0,p-\hat{y}} \hat{X}_p, \quad (8)$$

where $\hat{P}_{1,p} = |1\rangle_p \langle 1|_p$ and \hat{X}_p is the Pauli X operator acting on the qubit at plaquette p . It is interesting to note

that the plaquette operator at this truncation is a PXP term. PXP models have previously been studied as an effective Hamiltonian describing the low energy subspace of Rydberg atom arrays which can be described by Ising models [116–118]. It has been studied in the context of thermalization where the presence of scar states has been demonstrated [119–123]. Equation (8) can be described as a limit of an Ising model with fields in the \hat{x} and \hat{z} directions and that in this regime the Ising model has been shown to demonstrate confinement [124–126]. This suggests that it may be possible to connect the presence of confinement in the Ising model to the physics of large N_c Yang Mills.

There are three representations with $C \sim N_c$, namely, $p = 2$, $q = 2$, and $p = q = 1$, and the next truncation in the large N_c limit should include all three of those states. However, taking into account subleading N_c corrections, the representation with the second smallest Casimir at large N_c is the antisymmetric combination of two fundamental representations with $C = N_c - 1 - (2/N_c)$. Note that in SU(3), this is just the $\bar{\mathbf{3}}$ representation. Changing the truncation to include this representation allows neighboring plaquettes to be excited and includes states with vertices that have three incoming or outgoing $\mathbf{3}$ representations. As shown in more detail in the Supplemental Material [127], this truncation still fixes the representation on each link by the number of loops on the neighboring plaquettes, and each plaquette can still only be in the three possible states $|0\rangle$, $|\mathcal{U}\rangle$, and $|\mathcal{V}\rangle$. A pair of neighboring plaquettes can only be in one of the following states $|0\rangle|0\rangle$, $|0\rangle|\mathcal{U}\rangle$, $|\mathcal{U}\rangle|0\rangle$, $|0\rangle|\mathcal{V}\rangle$, $|\mathcal{V}\rangle|0\rangle$, $|\mathcal{U}\rangle|\mathcal{V}\rangle$, or $|\mathcal{V}\rangle|\mathcal{U}\rangle$. The Hilbert space is therefore still spanned by a qutrit at each plaquette.

At this truncation, the electric field operator on a link shared between plaquettes p and p' is given by

$$\hat{E}^2 = \frac{4}{3} [|\mathcal{U}\rangle_p \langle \mathcal{U}|_p + |\mathcal{U}\rangle_{p'} \langle \mathcal{U}|_{p'} + (|\mathcal{U}\rangle \leftrightarrow |\mathcal{V}\rangle)] \\ - \frac{4}{3} [|\mathcal{U}\rangle_p \langle \mathcal{U}|_p |\mathcal{U}\rangle_{p'} \langle \mathcal{U}|_{p'} + (|\mathcal{U}\rangle \leftrightarrow |\mathcal{V}\rangle)]. \quad (9)$$

The plaquette operator is given by

$$\hat{\square}_p = \sum_{c_k, s_i, s_f} \mathcal{M}_{c_1, c_2, c_3, c_4}^{s_i, s_f} \\ \times \hat{P}_{c_1, p-\hat{x}} \hat{P}_{c_2, p+\hat{x}} \hat{P}_{c_3, p-\hat{y}} \hat{P}_{c_4, p+\hat{y}} \\ \times (|s_f\rangle \langle s_i| + |s_i\rangle \langle s_f|). \quad (10)$$

Using results in the Supplemental Material, it can be seen that $\mathcal{M}_{0,0,0,0}^{s_i, s_f} = 1$ for all s_i and s_f , and when the controls are not all 0, $\mathcal{M}_{c_1, c_2, c_3, c_4}^{s_i, s_f} = 3^{-n_e/2}$ for transitions between allowed physical states where n_e is the number of excited neighboring plaquettes.

The Hamiltonians obtained at the two truncations discussed above have only negative off-diagonal elements. This means that their static properties can be studied using

Monte Carlo techniques without a sign problem [128,129]. This can be helpful for quantum simulation as classical MC calculations can be used to generate ensembles of states that when averaged produce a thermal distribution [130–134]. These states can be initialized on quantum computers which would allow for studying dynamics of this theory at finite temperature without a sign problem. Additionally, many of the variables used in scale setting in traditional lattice QCD are defined in terms of Euclidean correlation functions which are difficult to access on quantum computers [53,135–137]. For these truncated Hamiltonians, classical MC calculations can be used to compute these variables to set the scale for a simulation with the same Hamiltonian on a quantum computer [136].

To probe the effects of working to leading order in large N_c expansion, the electric vacuum was evolved in time on a 4×1 lattice with periodic boundary conditions (PBC). Figure 1 shows the evolution of $(1/T) \int_0^T dt \langle \psi(t) | \hat{H}_E | \psi(t) \rangle$ as a function of T for a SU(3) LGT truncated at $p + q \leq 1$. At long times, this observable is expected to equilibrate to a thermal value determined by the initial state's energy. As Fig. 1 shows, the relative error from the large N_c expansion is roughly 20% which should be expected from expanding in $(1/N_c)$ with $N_c = 3$.

As an example of how the formalism introduced in this work can be used for quantum simulation, the Hamiltonian in Eq. (8) was simulated on IBM's 133 qubit superconducting quantum computer *ibm_torino* [138,139].

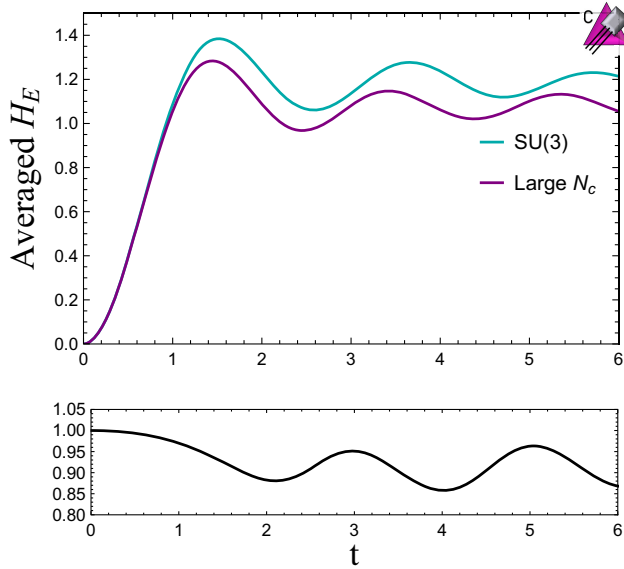


FIG. 1. Calculation of $(1/T) \int_0^T dt \langle \psi(t) | \hat{H}_E | \psi(t) \rangle$ on a 4×1 lattice with periodic boundary conditions and $g = 1$. The blue line shows the simulation for a SU(3) lattice gauge theory truncated at $p + q \leq 1$, using the formalism introduced in Ref. [48]. The purple line shows the time evolution computed with the large N_c truncated Hamiltonian in Eq. (8). The black line underneath shows the ratio of the large N_c electric energy to the SU(3) electric energy.

Because of the connectivity of the hardware, open boundary conditions were used. Time evolution was implemented using Trotterized time evolution operators. Errors in the calculation were suppressed using XX dynamical decoupling sequences and Pauli twirling [50,52,140,141]. Errors in the gates were mitigated using operator decoherence renormalization and CNOT noise extrapolations [50,52,79,141–146]. Readout errors were mitigated using twirled readout error extinction (T-REX) [147]. Since the number of Trotter steps that can be run on quantum hardware is limited, we utilize multiple time step sizes Δt to obtain results at more t values. Increasing Δt will increase the size of time discretization errors in the simulation, but this can be mitigated by choosing Δt such that late time slices are sampled by multiple values of Δt , which then allows an extrapolation to small Δt . The details of the implementation of these techniques are described in the Supplemental Material.

A 5×5 lattice with $g = 1$ was simulated using a set of 39 qubits on *ibm_torino*. Because of open boundary conditions, this lattice has 4×4 plaquettes. Sixteen of the qubits were used to represent the Hilbert space of the theory and the remaining qubits were used to enable efficient communication between them. The system was initialized in the electric vacuum and the probability of a qubit being excited averaged over the lattice is shown in Fig. 2 [148], showing results both from classical simulations of this relatively small system and from runs on quantum hardware using *ibm_torino*. We observe good agreement between the classical simulation and the results from *ibm_torino*. Note that this observable is proportional to the electric energy in the system, and previous work has used the evolution of the electric energy as a probe of thermalization times in SU(2) lattice gauge theory [150].

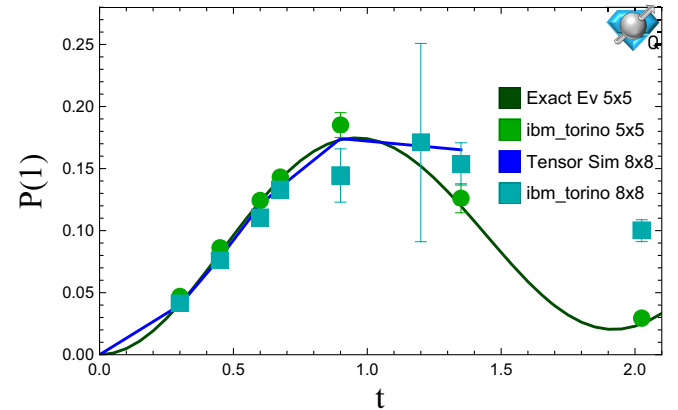


FIG. 2. Average probability of a plaquette being excited from the electric vacuum as a function of time on a 4×4 and 7×7 plaquette lattice with open boundary conditions and $g = 1$. The dark green points are an exact classical simulation. The dark blue points were obtained by tensor network simulations of up to two Trotter steps. The light blue and green points are the error mitigated results from *ibm_torino*.

Having validated the quantum circuits for the 5×5 lattice, an 8×8 lattice with open boundary conditions was simulated on `ibm_torino` as well. This requires 49 qubits to represent the state of the system and the remaining qubits are used to enable communication between them. The average probability of a plaquette being excited is shown in Fig. 2. Simulating the time evolution for a system of this size is beyond the reach of brute force state vector simulation. Vacuum properties of large one-dimensional systems can be simulated efficiently using tensor networks [151–155]; however, performing real time evolution requires resources that grow with evolution time. Scaling tensor network calculations to multiple spatial dimensions is practically challenging [156]. The dark blue points in Fig. 2 show tensor network simulations of up to two Trotter steps of the circuits that were implemented on `ibm_torino` using `cuQuantum` [157] on a single NVIDIA A100 GPU. Two Trotter steps took roughly one minute to run, however, three Trotter steps did not finish running within 20 h. For this reason, there is no extrapolation to $\Delta t = 0$ in the classical simulation or classical data for three Trotter steps. Because of the lack of the $\Delta t = 0$ extrapolation in the classical simulation and validation of the quantum circuits on a smaller lattice, it is expected that data from `ibm_torino` are a more accurate simulation of the dynamics of the system than the tensor network calculations. Note that further optimization of the classical simulation is likely to reduce the run-time; however, this system is still in the regime where classical simulation is expected to be difficult. For reference, running and processing all of the quantum circuits for a single time step took roughly 7 min.

In this work, a large N_c expansion was combined with electric basis truncations of the Kogut-Susskind Hamiltonian. This led to significant simplifications of the Hamiltonian and enabled a quantum simulation of SU(3) lattice gauge theory in multiple spatial dimensions. It is expected that this formalism can be extended to three spatial dimensions and to include matter. Going to sub-leading order in $1/N_c$ and to larger truncations should also be possible systematically. The simplifications from truncating at some order in $1/N_c$ and success of large N_c expansions may allow for near term simulations of phenomenologically relevant phenomena such as inelastic scattering, jet fragmentation, or thermalization. Additionally, the connection of the large N_c limit of SU(N_c) gauge theories to quantum gravity may allow quantum simulations of these truncations to give insights into some models of quantum gravity.

Acknowledgments—We would like to acknowledge helpful conversations with Ivan Burbano, Irian D’Andrea, Jesse Stryker, and Michael Kreshchuk. We would like to thank Martin Savage, Marc Illa, and Roland Farrell for many conversations related to quantum simulation. We would like to thank Aneesh Manohar for helpful discussions about

large N_c expansions. We would also like to acknowledge helpful conversations with Jad Halimeh about the emergence of PXP models from certain limits of gauge theories. This material is based upon work supported by the U.S. Department of Energy, Office of Science, National Quantum Information Science Research Centers, Quantum Systems Accelerator. Additional support is acknowledged from the U.S. Department of Energy (DOE), Office of Science under Contract No. DE-AC02-05CH11231, partially through Quantum Information Science Enabled Discovery (QuantISED) for High Energy Physics (KA2401032). This research used resources of the Oak Ridge Leadership Computing Facility (OLCF), which is a DOE Office of Science User Facility supported under Contract No. DE-AC05-00OR22725. We acknowledge the use of IBM Quantum services for this work. The views expressed are those of the authors, and do not reflect the official policy or position of IBM or the IBM Quantum team. This research used resources of the National Energy Research Scientific Computing Center, which is supported by the Office of Science of the U.S. Department of Energy under Contract No. DE-AC02-05CH11231.

-
- [1] K. G. Wilson, Confinement of quarks, *Phys. Rev. D* **10**, 2445 (1974).
 - [2] S. Borsanyi, S. Durr, Z. Fodor, C. Hoelbling, S. D. Katz, S. Krieg, L. Lellouch, T. Lippert, A. Portelli, K. K. Szabo, and B. C. Toth, *Ab initio* calculation of the neutron-proton mass difference, *Science* **347**, 1452 (2015).
 - [3] F. Karsch, K. Redlich, and A. Tawfik, Hadron resonance mass spectrum and lattice QCD thermodynamics, *Eur. Phys. J. C* **29**, 549 (2003).
 - [4] B. C. Tiburzi, M. L. Wagman, F. Winter, E. Chang, Z. Davoudi, W. Detmold, K. Orginos, M. J. Savage, and P. E. Shanahan (NPLQCD Collaboration), Double- β decay matrix elements from lattice quantum chromodynamics, *Phys. Rev. D* **96**, 054505 (2017).
 - [5] S. R. Beane, E. Chang, W. Detmold, K. Orginos, A. Parreño, M. J. Savage, and B. C. Tiburzi (NPLQCD Collaboration), *Ab initio* calculation of the $np \rightarrow d\gamma$ radiative capture process, *Phys. Rev. Lett.* **115**, 132001 (2015).
 - [6] M. J. Savage, P. E. Shanahan, B. C. Tiburzi, M. L. Wagman, F. Winter, S. R. Beane, E. Chang, Z. Davoudi, W. Detmold, and K. Orginos (NPLQCD Collaboration), Proton-proton fusion and tritium β decay from lattice quantum chromodynamics, *Phys. Rev. Lett.* **119**, 062002 (2017).
 - [7] G. D. Moore, Shear viscosity in QCD and why it’s hard to calculate, [arXiv:2010.15704](https://arxiv.org/abs/2010.15704).
 - [8] H.-L. Huang, D. Wu, D. Fan, and X. Zhu, Superconducting quantum computing: A review, *Sci. China Inf. Sci.* **63**, 180501 (2020).
 - [9] R. Bianchetti, S. Filipp, M. Baur, J. M. Fink, C. Lang, L. Steffen, M. Boissonneault, A. Blais, and A. Wallraff,

- Control and tomography of a three level superconducting artificial atom, *Phys. Rev. Lett.* **105**, 223601 (2010).
- [10] C. Wang, I. Gonin, A. Grassellino, S. Kazakov, A. Romanenko, V.P. Yakovlev, and S. Zorzetti, High-efficiency microwave-optical quantum transduction based on a cavity electro-optic superconducting system with long coherence time, *npj Quantum Inf.* **8**, 149 (2022).
- [11] A. Wallraff, D.I. Schuster, A. Blais, L. Frunzio, R.-S. Huang, J. Majer, S. Kumar, S.M. Girvin, and R.J. Schoelkopf, Strong coupling of a single photon to a superconducting qubit using circuit quantum electrodynamics, *Nature (London)* **431**, 162 (2004).
- [12] I. Chiorescu, P. Bertet, K. Semba, Y. Nakamura, C. J. P. M. Harmans, and J.E. Mooij, Coherent dynamics of a flux qubit coupled to a harmonic oscillator, *Nature (London)* **431**, 159 (2004).
- [13] C. D. Bruzewicz, J. Chiaverini, R. McConnell, and J. M. Sage, Trapped-ion quantum computing: Progress and challenges, *Appl. Phys. Rev.* **6**, 021314 (2019).
- [14] L. Henriët, L. Beguin, A. Signoles, T. Lahaye, A. Browaeys, G.-O. Reymond, and C. Jurczak, Quantum computing with neutral atoms, *Quantum* **4**, 327 (2020).
- [15] A. Browaeys and T. Lahaye, Many-body physics with individually controlled Rydberg atoms, *Nat. Phys.* **16**, 132 (2020).
- [16] D. Barredo, V. Lienhard, P. Scholl, S. de Lé séleuc, T. Boulier, A. Browaeys, and T. Lahaye, Three-dimensional trapping of individual Rydberg atoms in ponderomotive bottle beam traps, *Phys. Rev. Lett.* **124**, 023201 (2020).
- [17] D. Bluvstein, H. Levine, G. Semeghini, T. T. Wang, S. Ebadi, M. Kalinowski, A. Keesling, N. Maskara, H. Pichler, M. Greiner, V. Vuletić, and M.D. Lukin, A quantum processor based on coherent transport of entangled atom arrays, *Nature (London)* **604**, 451 (2022).
- [18] D. Bluvstein, S. J. Evered, A. A. Geim, S. H. Li, H. Zhou, T. Manovitz, S. Ebadi, M. Cain, M. Kalinowski, D. Hangleiter *et al.*, Logical quantum processor based on reconfigurable atom arrays, *Nature (London)* **626**, 58 (2023).
- [19] R. P. Feynman, Simulating physics with computers, *Int. J. Theor. Phys.* **21** (1981).
- [20] C. W. Bauer *et al.*, Quantum simulation for high-energy physics, *PRX Quantum* **4**, 027001 (2023).
- [21] T. S. Humble *et al.*, Snowmass white paper: Quantum computing systems and software for high-energy physics research, [arXiv:2203.07091](https://arxiv.org/abs/2203.07091).
- [22] T. S. Humble, G. N. Perdue, and M. J. Savage, Snowmass computational frontier: Topical group report on quantum computing, [arXiv:2209.06786](https://arxiv.org/abs/2209.06786).
- [23] D. Beck *et al.*, Quantum information science and technology for nuclear physics. input into U.S. long-range planning, 2023, [arXiv:2303.00113](https://arxiv.org/abs/2303.00113).
- [24] A. D. Meglio *et al.*, Quantum computing for high-energy physics: State of the art and challenges. Summary of the QC4HEP working group, *PRX Quantum* **5**, 037001 (2024).
- [25] M. A. Nielsen and I. L. Chuang, *Quantum Computation and Quantum Information: 10th Anniversary Edition*, 10th ed. (Cambridge University Press, New York, NY, USA, 2011).
- [26] A. Alexandru, P.F. Bedaque, S. Harmalkar, H. Lamm, S. Lawrence, and N.C. Warrington (NuQS Collaboration), Gluon field digitization for quantum computers, *Phys. Rev. D* **100**, 114501 (2019).
- [27] H. Lamm, S. Lawrence, and Y. Yamauchi (NuQS Collaboration), General methods for digital quantum simulation of gauge theories, *Phys. Rev. D* **100**, 034518 (2019).
- [28] Y. Ji, H. Lamm, and S. Zhu (NuQS Collaboration), Gluon field digitization via group space decimation for quantum computers, *Phys. Rev. D* **102**, 114513 (2020).
- [29] A. Alexandru, P.F. Bedaque, R. Brett, and H. Lamm, Spectrum of digitized QCD: Glueballs in a $S(1080)$ gauge theory, *Phys. Rev. D* **105**, 114508 (2022).
- [30] M. S. Alam, S. Hadfield, H. Lamm, and A. C. Y. Li (SQMS Collaboration), Primitive quantum gates for dihedral gauge theories, *Phys. Rev. D* **105**, 114501 (2022).
- [31] E. J. Gustafson, H. Lamm, F. Lovelace, and D. Musk, Primitive quantum gates for an $SU(2)$ discrete subgroup: Binary tetrahedral, *Phys. Rev. D* **106**, 114501 (2022).
- [32] T. V. Zache, D. González-Cuadra, and P. Zoller, Fermion-qudit quantum processors for simulating lattice gauge theories with matter, *Quantum* **7**, 1140 (2023).
- [33] D. González-Cuadra, T. V. Zache, J. Carrasco, B. Kraus, and P. Zoller, Hardware efficient quantum simulation of non-Abelian gauge theories with qudits on Rydberg platforms, *Phys. Rev. Lett.* **129**, 160501 (2022).
- [34] T. Byrnes and Y. Yamamoto, Simulating lattice gauge theories on a quantum computer, *Phys. Rev. A* **73**, 022328 (2006).
- [35] E. Zohar, J. I. Cirac, and B. Reznik, Simulating compact quantum electrodynamics with ultracold atoms: Probing confinement and nonperturbative effects, *Phys. Rev. Lett.* **109**, 125302 (2012).
- [36] E. Zohar, J. I. Cirac, and B. Reznik, Quantum simulations of gauge theories with ultracold atoms: Local gauge invariance from angular-momentum conservation, *Phys. Rev. A* **88**, 023617 (2013).
- [37] E. Zohar, J. I. Cirac, and B. Reznik, Cold-atom quantum simulator for $SU(2)$ Yang-Mills lattice gauge theory, *Phys. Rev. Lett.* **110**, 125304 (2013).
- [38] E. Zohar and M. Burrello, Formulation of lattice gauge theories for quantum simulations, *Phys. Rev. D* **91**, 054506 (2015).
- [39] E. Zohar, J. I. Cirac, and B. Reznik, Quantum simulations of lattice gauge theories using ultracold atoms in optical lattices, *Rep. Prog. Phys.* **79**, 014401 (2015).
- [40] E. Zohar, Quantum simulation of lattice gauge theories in more than one space dimension—requirements, challenges and methods, *Phil. Trans. R. Soc. A* **380**, 20210069 (2021).
- [41] I. Raychowdhury and J. R. Stryker, Solving Gauss's law on digital quantum computers with loop-string-hadron digitization, *Phys. Rev. Res.* **2**, 033039 (2020).
- [42] I. Raychowdhury and J. R. Stryker, Loop, string, and hadron dynamics in $SU(2)$ Hamiltonian lattice gauge theories, *Phys. Rev. D* **101**, 114502 (2020).
- [43] S. V. Kadam, I. Raychowdhury, and J. R. Stryker, Loop-string-hadron formulation of an $SU(3)$ gauge theory with dynamical quarks, *Phys. Rev. D* **107**, 094513 (2023).

- [44] A. F. Shaw, P. Lougovski, J. R. Stryker, and N. Wiebe, Quantum algorithms for simulating the lattice Schwinger model, *Quantum* **4**, 306 (2020).
- [45] A. Ciavarella, N. Klco, and M. J. Savage, Some conceptual aspects of operator design for quantum simulations of non-Abelian lattice gauge theories, [arXiv:2203.11988](https://arxiv.org/abs/2203.11988).
- [46] A. N. Ciavarella and I. A. Chernyshev, Preparation of the SU(3) lattice Yang-Mills vacuum with variational quantum methods, *Phys. Rev. D* **105**, 074504 (2022).
- [47] N. Klco, M. J. Savage, and J. R. Stryker, SU(2) non-Abelian gauge field theory in one dimension on digital quantum computers, *Phys. Rev. D* **101**, 074512 (2020).
- [48] A. Ciavarella, N. Klco, and M. J. Savage, Trailhead for quantum simulation of SU(3) Yang-Mills lattice gauge theory in the local multiplet basis, *Phys. Rev. D* **103**, 094501 (2021).
- [49] A. H. Z. Kavaki and R. Lewis, From square plaquettes to triamond lattices for SU(2) gauge theory, *Commun. Phys.* **7**, 208 (2024).
- [50] S. A. Rahman, R. Lewis, E. Mendicelli, and S. Powell, Real time evolution and a traveling excitation in SU(2) pure gauge theory on a quantum computer, *Proc. Sci., LATTICE2022* (2023) 025 [[arXiv:2210.11606](https://arxiv.org/abs/2210.11606)].
- [51] Y. Y. Atas, J. Zhang, R. Lewis, A. Jahanpour, J. F. Haase, and C. A. Muschik, SU(2) hadrons on a quantum computer via a variational approach, *Nat. Commun.* **12**, 6499 (2021).
- [52] S. A. Rahman, R. Lewis, E. Mendicelli, and S. Powell, Self-mitigating trotter circuits for SU(2) lattice gauge theory on a quantum computer, *Phys. Rev. D* **106**, 074502 (2022).
- [53] D. Paulson, L. Dellantonio, J. F. Haase, A. Celi, A. Kan, A. Jena, C. Kokail, R. van Bijnen, K. Jansen, P. Zoller, and C. A. Muschik, Simulating 2D effects in lattice gauge theories on a quantum computer, *PRX Quantum* **2**, 030334 (2021).
- [54] J. C. Halimeh, L. Homeier, A. Bohrdt, and F. Grusdt, Spin exchange-enabled quantum simulator for large-scale non-Abelian gauge theories, [arXiv:2305.06373](https://arxiv.org/abs/2305.06373).
- [55] Y. Meurice, Theoretical methods to design and test quantum simulators for the compact Abelian Higgs model, *Phys. Rev. D* **104**, 094513 (2021).
- [56] Z. Davoudi, M. Hafezi, C. Monroe, G. Pagano, A. Seif, and A. Shaw, Towards analog quantum simulations of lattice gauge theories with trapped ions, *Phys. Rev. Res.* **2**, 023015 (2020).
- [57] Z. Davoudi, I. Raychowdhury, and A. Shaw, Search for efficient formulations for Hamiltonian simulation of non-Abelian lattice gauge theories, *Phys. Rev. D* **104**, 074505 (2021).
- [58] R. Belyansky, S. Whitsitt, N. Mueller, A. Fahimniya, E. R. Bennewitz, Z. Davoudi, and A. V. Gorshkov, High-energy collision of quarks and hadrons in the schwinger model: From tensor networks to circuit QED, *Phys. Rev. Lett.* **132**, 091903 (2024).
- [59] D. Berenstein and H. Kawai, Integrable spin chains from large- n QCD at strong coupling, [arXiv:2308.11716](https://arxiv.org/abs/2308.11716).
- [60] M. Rigobello, G. Magnifico, P. Silvi, and S. Montangero, Hadrons in $(1 + 1)d$ Hamiltonian hardcore lattice QCD, [arXiv:2308.04488](https://arxiv.org/abs/2308.04488).
- [61] C. F. Kane, N. Gomes, and M. Kreshchuk, Nearly-optimal state preparation for quantum simulations of lattice gauge theories, *Phys. Rev. A* **110**, 012455 (2024).
- [62] S. Hariprakash, N. S. Modi, M. Kreshchuk, C. F. Kane, and C. W. Bauer, Strategies for simulating time evolution of Hamiltonian lattice field theories, [arXiv:2312.11637](https://arxiv.org/abs/2312.11637).
- [63] G.-X. Su, J. Osborne, and J. C. Halimeh, A cold-atom particle collider, [arXiv:2401.05489](https://arxiv.org/abs/2401.05489).
- [64] D. M. Grabowska, C. Kane, B. Nachman, and C. W. Bauer, Overcoming exponential scaling with system size in trotter-suzuki implementations of constrained Hamiltonians: $2 + 1$ u(1) lattice gauge theories, [arXiv:2208.03333](https://arxiv.org/abs/2208.03333).
- [65] C. W. Bauer and D. M. Grabowska, Efficient representation for simulating U(1) gauge theories on digital quantum computers at all values of the coupling, *Phys. Rev. D* **107**, L031503 (2023).
- [66] C. Kane, D. M. Grabowska, B. Nachman, and C. W. Bauer, Efficient quantum implementation of $2 + 1$ U(1) lattice gauge theories with gauss law constraints, [arXiv:2211.10497](https://arxiv.org/abs/2211.10497).
- [67] C. W. Bauer, I. D'Andrea, M. Freytsis, and D. M. Grabowska, A new basis for Hamiltonian SU(2) simulations, *Phys. Rev. D* **109**, 074501 (2024).
- [68] E. A. Martinez, C. A. Muschik, P. Schindler, D. Nigg, A. Erhard, M. Heyl, P. Hauke, M. Dalmonte, T. Monz, P. Zoller, and R. Blatt, Real-time dynamics of lattice gauge theories with a few-qubit quantum computer, *Nature (London)* **534**, 516 (2016).
- [69] M. Illa and M. J. Savage, Basic elements for simulations of standard model physics with quantum annealers: Multigrid and clock states, *Phys. Rev. A* **106**, 052605 (2022).
- [70] R. C. Farrell, I. A. Chernyshev, S. J. M. Powell, N. A. Zemlevskiy, M. Illa, and M. J. Savage, Preparations for quantum simulations of quantum chromodynamics in $1 + 1$ dimensions. I. Axial gauge, *Phys. Rev. D* **107**, 054512 (2023).
- [71] R. C. Farrell, I. A. Chernyshev, S. J. M. Powell, N. A. Zemlevskiy, M. Illa, and M. J. Savage, Preparations for quantum simulations of quantum chromodynamics in $1 + 1$ dimensions. II. Single-baryon β -decay in real time, *Phys. Rev. D* **107**, 054513 (2023).
- [72] Y. Y. Atas, J. F. Haase, J. Zhang, V. Wei, S. M. L. Pfaendler, R. Lewis, and C. A. Muschik, Simulating one-dimensional quantum chromodynamics on a quantum computer: Real-time evolutions of tetra- and pentaquarks, *Phys. Rev. Res.* **5**, 033184 (2023).
- [73] B. Yang, H. Sun, R. Ott, H.-Y. Wang, T. V. Zache, J. C. Halimeh, Z.-S. Yuan, P. Hauke, and J.-W. Pan, Observation of gauge invariance in a 71-site Bose-Hubbard quantum simulator, *Nature (London)* **587**, 392 (2020).
- [74] Z.-Y. Zhou, G.-X. Su, J. C. Halimeh, R. Ott, H. Sun, P. Hauke, B. Yang, Z.-S. Yuan, J. Berges, and J.-W. Pan, Thermalization dynamics of a gauge theory on a quantum simulator, *Science* **377**, 311 (2022).
- [75] G.-X. Su, H. Sun, A. Hudomal, J.-Y. Desaules, Z.-Y. Zhou, B. Yang, J. C. Halimeh, Z.-S. Yuan, Z. Papić, and J.-W. Pan, Observation of many-body scarring in a Bose-Hubbard quantum simulator, *Phys. Rev. Res.* **5**, 023010 (2023).
- [76] W.-Y. Zhang, Y. Liu, Y. Cheng, M.-G. He, H.-Y. Wang, T.-Y. Wang, Z.-H. Zhu, G.-X. Su, Z.-Y. Zhou, Y.-G. Zheng,

- H. Sun, B. Yang, P. Hauke, W. Zheng, J. C. Halimeh, Z.-S. Yuan, and J.-W. Pan, Observation of microscopic confinement dynamics by a tunable topological θ -angle, [arXiv:2306.11794](#).
- [77] J. Mildenerger, W. Mruzekiewicz, J. C. Halimeh, Z. Jiang, and P. Hauke, Probing confinement in a \mathbb{Z}_2 lattice gauge theory on a quantum computer, [arXiv:2203.08905](#).
- [78] A. N. Ciavarella, Quantum simulation of lattice QCD with improved Hamiltonians, *Phys. Rev. D* **108**, 094513 (2023).
- [79] R. C. Farrell, M. Illa, A. N. Ciavarella, and M. J. Savage, Scalable circuits for preparing ground states on digital quantum computers: The Schwinger model vacuum on 100 qubits, *PRX Quantum* **5**, 020315 (2024).
- [80] R. C. Farrell, M. Illa, A. N. Ciavarella, and M. J. Savage, Quantum simulations of hadron dynamics in the Schwinger model using 112 qubits, *Phys. Rev. D* **109**, 114510 (2024).
- [81] C. Charles, E. J. Gustafson, E. Hardt, F. Herren, N. Hogan, H. Lamm, S. Starecheski, R. S. V. de Water, and M. L. Wagman, Simulating \mathbb{Z}_2 lattice gauge theory on a quantum computer, *Phys. Rev. E* **109**, 015307 (2024).
- [82] N. Mueller, J. A. Carolan, A. Connelly, Z. Davoudi, E. F. Dumitrescu, and K. Yeter-Aydeniz, Quantum computation of dynamical quantum phase transitions and entanglement tomography in a lattice gauge theory, *PRX Quantum* **4**, 030323 (2023).
- [83] B. Lucini and M. Panero, SU(N) gauge theories at large N, *Phys. Rep.* **526**, 93 (2013).
- [84] A. V. Manohar, Large N QCD, in *Les Houches Summer School in Theoretical Physics, Session 68: Probing the Standard Model of Particle Interactions* (1998) pp. 1091–1169, [arXiv:hep-ph/9802419](#).
- [85] T. Sjostrand, S. Mrenna, and P. Z. Skands, PYTHIA 6.4 physics and manual, *J. High Energy Phys.* **05** (2006) 026.
- [86] M. Bahr *et al.*, HERWIG++ physics and manual, *Eur. Phys. J. C* **58**, 639 (2008).
- [87] G. 't Hooft, A planar diagram theory for strong interactions, *Nucl. Phys.* **B72**, 461 (1974).
- [88] A. PICH, Colourless mesons in a polychromatic world, in *Phenomenology of Large Nc QCD* (World Scientific, Singapore, 2002).
- [89] D. B. Kaplan and M. J. Savage, The spin-flavor dependence of nuclear forces from large-N QCD, *Phys. Lett. B* **365**, 244 (1996).
- [90] J. Maldacena, The large-N limit of superconformal field theories and supergravity, *Int. J. Theor. Phys.* **38**, 1113 (1999).
- [91] E. Witten, The $1/n$ expansion in atomic and particle physics, in *Recent Developments in Gauge Theories*, edited by G. Hooft, C. Itzykson, A. Jaffe, H. Lehmann, P. K. Mitter, I. M. Singer, and R. Stora (Springer US, Boston, MA, 1980), pp. 403–419.
- [92] L. G. Yaffe, Large N limits as classical mechanics, *Rev. Mod. Phys.* **54**, 407 (1982).
- [93] A. Jevicki, O. Karim, J. Rodrigues, and H. Levine, Loop space Hamiltonians and numerical methods for large-N gauge theories, *Nucl. Phys.* **B213**, 169 (1983).
- [94] A. Jevicki, O. Karim, J. Rodrigues, and H. Levine, Loop-space Hamiltonians and numerical methods for large-N gauge theories (II), *Nucl. Phys.* **B230**, 299 (1984).
- [95] J. B. Kogut, An introduction to lattice gauge theory and spin systems, *Rev. Mod. Phys.* **51**, 659 (1979).
- [96] T. Banks, S. Raby, L. Susskind, J. Kogut, D. R. T. Jones, P. N. Scharbach, and D. K. Sinclair, Strong-coupling calculations of the hadron spectrum of quantum chromodynamics, *Phys. Rev. D* **15**, 1111 (1977).
- [97] D. Jones, R. Kenway, J. Kogut, and D. Sinclair, Lattice gauge theory calculations using an improved strong-coupling expansion and matrix padé approximants, *Nucl. Phys.* **B158**, 102 (1979).
- [98] J. Kogut and L. Susskind, Hamiltonian formulation of Wilson's lattice gauge theories, *Phys. Rev. D* **11**, 395 (1975).
- [99] T. V. Zache, D. González-Cuadra, and P. Zoller, Quantum and classical spin-network algorithms for q -deformed Kogut-Susskind gauge theories, *Phys. Rev. Lett.* **131**, 171902 (2023).
- [100] T. Hayata and Y. Hidaka, q deformed formulation of Hamiltonian SU(3) Yang-Mills theory, *J. High Energy Phys.* **09** (2023) 123.
- [101] Z. Davoudi, A. F. Shaw, and J. R. Stryker, General quantum algorithms for Hamiltonian simulation with applications to a non-Abelian lattice gauge theory, *Quantum* **7**, 1213 (2023).
- [102] M. A. Levin and X.-G. Wen, String-net condensation: A physical mechanism for topological phases, *Phys. Rev. B* **71**, 045110 (2005).
- [103] M. C. Bañuls, K. Cichy, J. I. Cirac, K. Jansen, and S. Kühn, Efficient basis formulation for $(1 + 1)$ -dimensional SU(2) lattice gauge theory: Spectral calculations with matrix product states, *Phys. Rev. X* **7**, 041046 (2017).
- [104] J. F. Haase, L. Dellantonio, A. Celi, D. Paulson, A. Kan, K. Jansen, and C. A. Muschik, A resource efficient approach for quantum and classical simulations of gauge theories in particle physics, *Quantum* **5**, 393 (2021).
- [105] F. Bruckmann, K. Jansen, and S. Kühn, O(3) nonlinear sigma model in $1 + 1$ dimensions with matrix product states, *Phys. Rev. D* **99**, 074501 (2019).
- [106] T. V. Zache, M. Van Damme, J. C. Halimeh, P. Hauke, and D. Banerjee, Toward the continuum limit of a $(1 + 1)$ D quantum link Schwinger model, *Phys. Rev. D* **106**, L091502 (2022).
- [107] A. Alexandru, P. F. Bedaque, A. Carosso, M. J. Cervia, and A. Sheng, Qubitization strategies for bosonic field theories, *Phys. Rev. D* **107**, 034503 (2023).
- [108] J. Y. Araz, S. Schenk, and M. Spannowsky, Toward a quantum simulation of nonlinear sigma models with a topological term, *Phys. Rev. A* **107**, 032619 (2023).
- [109] H. Liu, T. Bhattacharya, S. Chandrasekharan, and R. Gupta, Phases of 2D massless QCD with qubit regularization, [arXiv:2312.17734](#).
- [110] B. Müller and X. Yao, Simple Hamiltonian for quantum simulation of strongly coupled $(2 + 1)$ D SU(2) lattice gauge theory on a honeycomb lattice, *Phys. Rev. D* **108**, 094505 (2023).
- [111] L. Ebner, A. Schäfer, C. Seidl, B. Müller, and X. Yao, Eigenstate thermalization in $(2 + 1)$ -dimensional SU(2) lattice gauge theory, *Phys. Rev. D* **109**, 014504 (2024).

- [112] X. Yao, SU(2) gauge theory in $2 + 1$ dimensions on a plaquette chain obeys the eigenstate thermalization hypothesis, *Phys. Rev. D* **108**, L031504 (2023).
- [113] X. Yao, L. Ebner, B. Müller, A. Schäfer, and C. Seidl, Testing eigenstate thermalization hypothesis for non-Abelian gauge theories, *EPJ Web Conf.* **296**, 13008 (2024).
- [114] L. Ebner, A. Schäfer, C. Seidl, B. Müller, and X. Yao, Entanglement entropy of $(2 + 1)$ -dimensional SU(2) lattice gauge theory, *Phys. Rev. D* **110**, 014505 (2024).
- [115] F. Turro, A. Ciavarella, and X. Yao, Classical and quantum computing of shear viscosity for $2 + 1$ D SU(2) gauge theory, *Phys. Rev. D* **109**, 114511 (2024).
- [116] S. Ebadi, T.T. Wang, H. Levine, A. Keesling, G. Semeghini, A. Omran, D. Bluvstein, R. Samajdar, H. Pichler, W.W. Ho, S. Choi, S. Sachdev, M. Greiner, V. Vuletić, and M.D. Lukin, Quantum phases of matter on a 256-atom programmable quantum simulator, *Nature (London)* **595**, 227 (2021).
- [117] G. Semeghini, H. Levine, A. Keesling, S. Ebadi, T.T. Wang, D. Bluvstein, R. Verresen, H. Pichler, M. Kalinowski, R. Samajdar, A. Omran, S. Sachdev, A. Vishwanath, M. Greiner, V. Vuletić, and M.D. Lukin, Probing topological spin liquids on a programmable quantum simulator, *Science* **374**, 1242 (2021).
- [118] A. Omran, H. Levine, A. Keesling, G. Semeghini, T.T. Wang, S. Ebadi, H. Bernien, A.S. Zibrov, H. Pichler, S. Choi, J. Cui, M. Rossignolo, P. Rembold, S. Montangero, T. Calarco, M. Endres, M. Greiner, V. Vuletić, and M.D. Lukin, Generation and manipulation of Schrödinger cat states in Rydberg atom arrays, *Science* **365**, 570 (2019).
- [119] R. Nandkishore and D.A. Huse, Many-body localization and thermalization in quantum statistical mechanics, *Annu. Rev. Condens. Matter Phys.* **6**, 15 (2015).
- [120] S. Choi, C.J. Turner, H. Pichler, W.W. Ho, A.A. Michailidis, Z. Papić, M. Serbyn, M.D. Lukin, and D.A. Abanin, Emergent SU(2) dynamics and perfect quantum many-body scars, *Phys. Rev. Lett.* **122**, 220603 (2019).
- [121] S. Moudgalya, B.A. Bernevig, and N. Regnault, Quantum many-body scars and hilbert space fragmentation: A review of exact results, *Rep. Prog. Phys.* **85**, 086501 (2022).
- [122] A. Chandran, T. Iadecola, V. Khemani, and R. Moessner, Quantum many-body scars: A quasiparticle perspective, *Annu. Rev. Condens. Matter Phys.* **14**, 443 (2023).
- [123] F.M. Surace, P.P. Mazza, G. Giudici, A. Lerose, A. Gambassi, and M. Dalmonte, Lattice gauge theories and string dynamics in Rydberg atom quantum simulators, *Phys. Rev. X* **10**, 021041 (2020).
- [124] M. Kormos, M. Collura, G. Takács, and P. Calabrese, Real-time confinement following a quantum quench to a non-integrable model, *Nat. Phys.* **13**, 246 (2016).
- [125] A.J.A. James, R.M. Konik, and N.J. Robinson, Non-thermal states arising from confinement in one and two dimensions, *Phys. Rev. Lett.* **122**, 130603 (2019).
- [126] N.J. Robinson, A.J.A. James, and R.M. Konik, Signatures of rare states and thermalization in a theory with confinement, *Phys. Rev. B* **99**, 195108 (2019).
- [127] See Supplemental Material at <http://link.aps.org/supplemental/10.1103/PhysRevLett.133.111901> for addition details for the calculations performed in this paper.
- [128] S. Bravyi, D.P. DiVincenzo, R.I. Oliveira, and B.M. Terhal, The complexity of stoquastic local Hamiltonian problems, [arXiv:quant-ph/0606140](https://arxiv.org/abs/quant-ph/0606140).
- [129] S. Suzuki, J.-i. Inoue, B.K. Chakrabarti, S. Suzuki, J.-i. Inoue, and B.K. Chakrabarti, Transverse Ising system in higher dimensions (pure systems), *Quantum Ising Phases and Transitions in Transverse Ising Models*, 47 (2013).
- [130] H. Lamm and S. Lawrence, Simulation of nonequilibrium dynamics on a quantum computer, *Phys. Rev. Lett.* **121**, 170501 (2018).
- [131] S. Harmalkar, H. Lamm, and S. Lawrence, Quantum simulation of field theories without state preparation, [arXiv:2001.11490](https://arxiv.org/abs/2001.11490).
- [132] E.J. Gustafson and H. Lamm, Toward quantum simulations of z_2 gauge theory without state preparation, *Phys. Rev. D* **103**, 054507 (2021).
- [133] N.S. Blunt, T.W. Rogers, J.S. Spencer, and W.M.C. Foulkes, Density-matrix quantum Monte Carlo method, *Phys. Rev. B* **89**, 245124 (2014).
- [134] J. Saroni, H. Lamm, P.P. Orth, and T. Iadecola, Reconstructing thermal quantum quench dynamics from pure states, *Phys. Rev. B* **108**, 134301 (2023).
- [135] R. Sommer, Scale setting in lattice QCD, *Proc. Sci., LATTICE2013 (2014)* 015 [[arXiv:1401.3270](https://arxiv.org/abs/1401.3270)].
- [136] G. Clemente, A. Crippa, and K. Jansen, Strategies for the determination of the running coupling of $(2 + 1)$ -dimensional QED with quantum computing, *Phys. Rev. D* **106**, 114511 (2022).
- [137] A.N. Ciavarella, S. Caspar, H. Singh, and M.J. Savage, Preparation for quantum simulation of the $(1 + 1)$ -dimensional O(3) nonlinear σ model using cold atoms, *Phys. Rev. A* **107**, 042404 (2023).
- [138] G. Aleksandrowicz, T. Alexander, P. Barkoutsos, L. Bello, Y. Ben-Haim, D. Bucher, F.J. Cabrera-Hernández, J. Carballo-Franquis, A. Chen, C.-F. Chen *et al.*, Qiskit: An open-source framework for quantum computing, Accessed on: Mar 16 (2019).
- [139] IBM Quantum Experience, *ibm_torino v1.0.2*, <https://quantum-computing.ibm.com> (2023).
- [140] L. Viola, E. Knill, and S. Lloyd, Dynamical decoupling of open quantum systems, *Phys. Rev. Lett.* **82**, 2417 (1999).
- [141] M. Urbanek, B. Nachman, V.R. Pascuzzi, A. He, C.W. Bauer, and W.A. de Jong, Mitigating depolarizing noise on quantum computers with noise-estimation circuits, *Phys. Rev. Lett.* **127**, 270502 (2021).
- [142] M. Asaduzzaman, R.G. Jha, and B. Sambahivam, Sachdev-Ye-Kitaev model on a noisy quantum computer, *Phys. Rev. D* **109**, 105002 (2024).
- [143] L. Hidalgo and P. Draper, Quantum simulations for strong-field QED, *Phys. Rev. D* **109**, 076004 (2024).
- [144] O. Kiss, M. Grossi, and A. Roggero, Quantum error mitigation for fourier moment computation, [arXiv:2401.13048](https://arxiv.org/abs/2401.13048).
- [145] A. He, B. Nachman, W.A. de Jong, and C.W. Bauer, Zero-noise extrapolation for quantum-gate error mitigation with identity insertions, *Phys. Rev. A* **102**, 012426 (2020).

- [146] V. R. Pascuzzi, A. He, C. W. Bauer, W. A. de Jong, and B. Nachman, Computationally efficient zero-noise extrapolation for quantum-gate-error mitigation, *Phys. Rev. A* **105**, 042406 (2022).
- [147] E. van den Berg, Z. K. Mineev, and K. Temme, Model-free readout-error mitigation for quantum expectation values, *Phys. Rev. A* **105**, 032620 (2022).
- [148] The icons in the corners of plots indicate if classical or quantum compute resources were used to perform the calculation [149] and are available at <https://iqus.uw.edu/resources/icons/>.
- [149] N. Klco and M. J. Savage, Minimally entangled state preparation of localized wave functions on quantum computers, *Phys. Rev. A* **102**, 012612 (2020).
- [150] T. Hayata and Y. Hidaka, Thermalization of Yang-Mills theory in a $(3 + 1)$ -dimensional small lattice system, *Phys. Rev. D* **103**, 094502 (2021).
- [151] S. R. White, Density matrix formulation for quantum renormalization groups, *Phys. Rev. Lett.* **69**, 2863 (1992).
- [152] S. R. White, Density-matrix algorithms for quantum renormalization groups, *Phys. Rev. B* **48**, 10345 (1993).
- [153] F. Verstraete, J. J. García-Ripoll, and J. I. Cirac, Matrix product density operators: Simulation of finite-temperature and dissipative systems, *Phys. Rev. Lett.* **93**, 207204 (2004).
- [154] J. Haegeman, J. I. Cirac, T. J. Osborne, I. Pižorn, H. Verschelde, and F. Verstraete, Time-dependent variational principle for quantum lattices, *Phys. Rev. Lett.* **107**, 070601 (2011).
- [155] J. Haegeman, C. Lubich, I. Oseledets, B. Vandereycken, and F. Verstraete, Unifying time evolution and optimization with matrix product states, *Phys. Rev. B* **94**, 165116 (2016).
- [156] Y. Pang, T. Hao, A. Dugad, Y. Zhou, and E. Solomonik, Efficient 2D tensor network simulation of quantum systems, [arXiv:2006.15234](https://arxiv.org/abs/2006.15234).
- [157] NVIDIA cuQuantum team, NVIDIA/cuQuantum: cuQuantum v23.10 (2023).
- [158] Note that this presentation only works as presented in the simplest topological sector of the allowed states. There are other states that allow for additional overall winding numbers, which will not be considered in this work. One can easily generalize the loop representation to also include winding loops.
- [159] D. Weingarten, Asymptotic behavior of group integrals in the limit of infinite rank, *J. Math. Phys. (N.Y.)* **19**, 999 (2008).

End Matter

Appendix A: Graphical representation of basis states—To explain the large N_c counting employed in this work, it will be useful to develop some graphical notation for physical states on a lattice. The Hilbert space describing a single link in a lattice gauge theory is spanned by electric basis states of the form $|R, a, b\rangle$ where R is a representation of the gauge group, and a and b are indices that label states in the representation R when acted from the left and right. Physical states are subject to a constraint from Gauss’s law which requires that the sum of representations on each vertex of the lattice forms a singlet. On a lattice where each vertex is connected to at most three links, gauge invariant states can be specified by the representation R on each link and a specification on each vertex of how the links add to form a singlet.

For $SU(N)$ gauge groups, a representation R can be labeled by a Young diagram, which can be specified through the number of columns with 1, 2, \dots , $N - 1$ boxes. For $SU(3)$ only two numbers are required, and the labels are often chosen as (p, q) , with p labeling the number of columns with a single box, and q labeling the number of columns with two boxes. It will be useful to obtain a

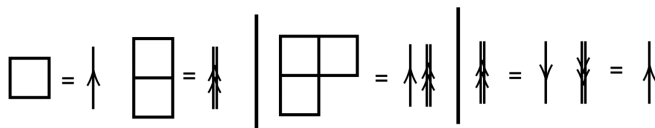


FIG. 3. Graphical representations of Young diagrams in terms of arrows.

representation of Young diagrams in terms of lines with arrows, as illustrated in Fig. 3. One can see that fundamental and antifundamental representations can be represented either by lines with a single arrow in one direction, or by lines with a double arrow in the opposite direction. More complex representations can be built by combining such lines together.

For lattices where vertices connect to more links, such as a square lattice in 2D or 3D, not all states that can be labeled by the representation above are linearly independent, leading to an ambiguity in labeling the basis states. This is due to the so-called Mandelstam constraints, which relate contractions of representation indices across a vertex. A point splitting procedure can be performed to split each vertex into three link vertices connected by virtual links, which lifts this ambiguity. In this point-split lattice, the gauge invariant states can be specified with the same assignment of labels used on a trivalent lattice.

There is an equivalent labeling of the states of the physical Hilbert space that will prove useful, using the arrow representation introduced above. This is illustrated in Fig. 4, and will be called a “loop representation” [158]. In this representation each state is labeled by a set of loops L_i , together with a specification a_ℓ , which denotes the way the arrows at each link ℓ having more than one loop pass through being combined. Each loop needs to specify which plaquettes are encircled and in which order, while a_ℓ contains the information on how to combine lines of multiple loops into single or double arrows. Note that it might seem that there is an ambiguity in the choice of single arrows in one or double arrows in the other direction. This

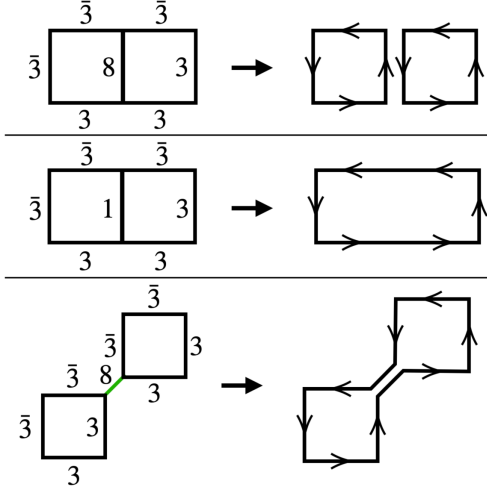


FIG. 4. Graphical representations of basis states on a point-split lattice.

ambiguity is fixed by choosing representations with $p = 0$ or $q = 0$ to have only single arrows, and demanding that the number of arrows entering and leaving a vertex is conserved. Because of the point splitting, closed loops have the property that their lines cannot cross each other, so they cannot form knots or be twisted. A loop representation is therefore spanned by the states $|\{L_i, a_\ell\}\rangle$. Note that this loop representation is simply a graphical representation of the states with definite representation at each link. In particular, lines do not necessarily represent the tensor indices of a given representation, and lines being connected does not necessarily imply tensor indices being contracted. Before moving on, we want to make it clear that the loop representation as given is likely not a computationally efficient representation of the Hilbert space, since loops are necessarily nonlocal objects which can in general span an arbitrary number of plaquettes. Its usefulness will come from when applying the $1/N_c$ expansion.

The vacuum state in the interacting theory can be generated adiabatically from the vacuum state of the free electric theory (the vacuum at $g = \infty$) by acting with the operators of the interacting Hamiltonian, which are $\hat{\square}$

operators at the different plaquettes or \hat{E}_i^2 operators at the different links. Excited states in the simplest topological sector can be obtained by further applications of electric energy or plaquette operators. One can therefore classify all states in this sector by the minimum number of plaquette operators and its conjugate that are required to reach it from the vacuum

$$|\{P_p, \bar{P}_p\}\rangle \equiv \prod_p \hat{\square}_p^{P_p} \hat{\square}_p^{\dagger \bar{P}_p} |0\rangle. \quad (\text{A1})$$

This state will be a linear combination of several electric basis states and one can write

$$|\{P_p, \bar{P}_p\}\rangle = \sum_{\{L_i, a_\ell\}} \langle \{L_i, a_\ell\} | \{P_p, \bar{P}_p\} \rangle |L_i, a_\ell\rangle. \quad (\text{A2})$$

Appendix B: Large N_c counting of states—The large N_c scaling of a state, $|\{L_i, a_\ell\}\rangle$ is determined by the large N_c expansion of $\langle \{L_i, a_\ell\} | \{P_p, \bar{P}_p\} \rangle$ for the minimal choice of P_p and \bar{P}_p to obtain a nonzero overlap. Defining $|\{L_i\}\rangle = \prod_i U_{L_i} |0\rangle$ where U_{L_i} is a product of parallel transporters along the loop L_i and using that the overlap $\langle \{L_i, a_\ell\} | \{L_i\} \rangle$ is $\mathcal{O}(1)$ in the N_c scaling, the N_c scaling is determined by the overlap $\langle \{L_i\} | \{P_p, \bar{P}_p\} \rangle$. This overlap can be evaluated in the magnetic basis through inserting $\mathbf{1} = \prod_{\text{links } l} \int dU_l |U_l\rangle \langle U_l|$. To evaluate the large N_c scaling of these integrals, the identity

$$\int dU \prod_{n=1}^q U_{i_n j_n} U_{i'_n j'_n}^* = \frac{1}{N_c^q} \sum_{\text{permutations } k} \prod_{n=1}^q \delta_{i_n i'_{k_n}} \delta_{j_n j'_{k_n}} + \mathcal{O}\left(\frac{1}{N_c^{q+1}}\right), \quad (\text{B1})$$

will be used [159]. The large N_c scaling will be determined by the permutation of indices contraction that gives the largest factors of N_c . A diagrammatic method of evaluating the large N_c scaling is shown in Fig. 5.

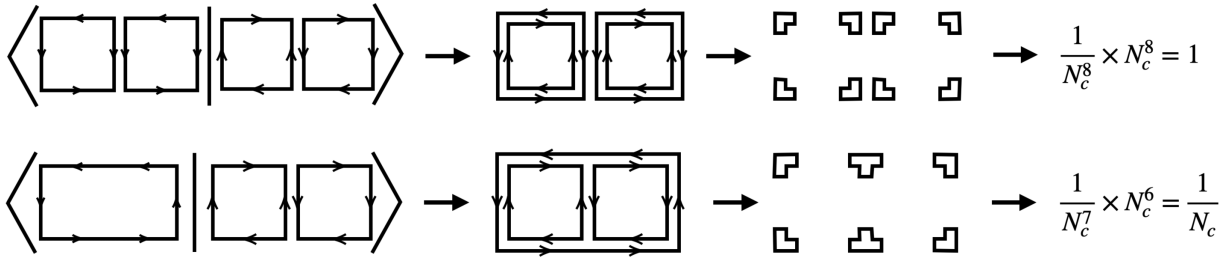


FIG. 5. Graphical method to obtain the scaling of the overlap matrix $\langle \{L_i\} | \{P_p, \bar{P}_p\} \rangle$. The top example contains two loops, each encircling a single plaquette $m_1 = m_2 = 1$, while the bottom example has a single loop encircling 2 loops $m_1 = 1$. This gives for the top example $q_1 = q_2 = 1 + 3 \times 1 = 4$ and $v_1 = v_2 = 2 + 2 \times 1 = 4$, giving the final scaling N_c^0 . For the bottom example we have $q_1 = 1 + 2 \times 3 = 7$ and $v_1 = 2 + 2 \times 2 = 6$, giving the final scaling $1/N_c$.

First, the plaquette operators being applied are placed over loops in the final state. To determine the powers of N_c that come from contracting the Kronecker δ 's, one can erase the middle of each link in the diagram and connect the lines from the same vertex. This leaves a set of v closed loops involving one vertex each, and each of these closed loops contributes a factor of N_c in the numerator. Each loop L_i therefore contributes a factor $N_c^{v_i - q_i}$ and the total N_c scaling is given by

$$N_c^{v-q}, \quad q \equiv \sum_i q_i, \quad v \equiv \sum_i v_i \quad (\text{B2})$$

to the final overlap. Since each U_{ij} in Eq. (B1) corresponds to a line in the figure, one immediately finds that $q = n_l/2$, where n_l is the total number of lines on each link in the diagram. Denoting by m_i the number of plaquettes encircled by each loop L_i , one needs m_i plaquette operators for each loop. The total number of lines is then given by $n_l = 2 + 6m_i$, and the total number of closed loops n_v is

given by $2 + 2m_i$ for each loop in the basis. Thus one finds

$$q_i = 1 + 3m_i, \quad v_i = 2 + 2m_i. \quad (\text{B3})$$

Putting this together, one finds that each loop contributes a factor of $N_c^{1-m_i}$ to the overall scaling of the overlap, such that

$$\langle \{L_i, a_\ell\} | \{P_p, \bar{P}_p\} \rangle \propto \prod_i N_c^{1-m_i}. \quad (\text{B4})$$

This implies that the states that can be reached to leading order in $1/N_c$ are those that only involve loops L_i with $m_i = 1$. Therefore, the only overlap that survives in the large N_c limit is the one with states $|\{L_i, a_\ell\}\rangle$ for which each loop encircles exactly one plaquette. At order $1/N_c$, states with loops extending over two plaquettes will be present. Basis constructions similar to those in the main text can be used to represent these states on a quantum computer.